Research Article

Journal of Physical Organic Chemistry

Received: 31 March 2010, Revised: 15 August 2010, Accepted: 25 August 2010, Published online in Wiley Online Library: 22 October 2010

(wileyonlinelibrary.com) DOI 10.1002/poc.1799

Structural and property comparison between the di-piperidinyl- and di-pyrrolidinyl-substituted perylene tetracarboxylic diimides

Junqian Feng[a,b], Delou Wang[a], Hailong Wang[a], Daopeng Zhang[a], Liangliang Zhang[a] and Xiyou Li[a]*

Four compounds 1–4 connected with cyclic amino groups at the bay positions of perylenetetracarboxylic diimide (PDI) have been prepared and the isomers with 1,7- and 1,6-substituted PDIs were successfully separated by conventional column chromatography. The structures of 1,7-dipyrrolidinyl-substituted PDI (1) and 1,7-dipiperidinyl-substituted PDI (3) were further characterized by single crystal X-ray diffraction experiments. The crystal structure revealed that the small difference in the molecular structure has caused significant difference on the absorption and emission spectra as well as the electrochemical properties. The shorter bond length of C1—N3, together with the more sp2 hybrid atomic orbital characteristics of the nitrogen atom in pyrrolidine relative to those in piperidine is found to be responsible for this large property difference between 1 and 3. Copyright © 2010 John Wiley & Sons, Ltd.

Supporting information may be found in the online version of this paper.

Keywords: crystal structure; perylene tetracarboxylic diimide; photophysical properties; pyrrolidine; piperidine

INTRODUCTION

Perylenetetracarboxylic diimides (PDIs) have attracted much interest and found wide range applications in diverse fields of current research because of their excellent thermal- and photostability, high luminescence efficiency, and novel opto-electronic properties.[1–4] Because the low solubility of PDIs in conventional organic solvents always induces difficulties on the synthesis and purification, bay substitution is recently popularly employed as an efficient way to improve the solubility of PDI compounds. Furthermore, bay substitution has been found to be very efficient on varying the physical properties of PDIs. Therefore, developing new PDI compounds for different particular applications by introducing different side groups at bay positions has attracted a lot of attention in the past decade. Amino group substituted PDIs represent a very important category of these PDIs derivatives, which are characterized with their blue–green color, long wavelength absorption and emission, as well as environmental sensitive photophysical property. The application researches of these compounds as photosensitizers in photodynamic therapy,[5] molecular switches,[6] light-harvesting antenna arrays,[7,8] and dye sensitized solar cell,[9–12] and other functional materials have been reported in literatures.[13–30]

1,7-Dipyrrolidinyl- or piperidinyl-substituted PDIs had been prepared firstly by Wasielewski in 1999 by the nucleophilic substitution of 1,7-dibromo PDI by pyrrolidine or piperidine, respectively.[31] Because 1,7-dibromo PDI is always contaminated with 1,6-dibromo isomer, which cannot be separated by column chromatography, the nucleophilic substitution of dibromo PDI by pyrrolidine or piperidine leads inevitably to the formation of a mixture of 1,7 and 1,6 isomers.[32] Fortunately, these two isomers can be separated by column chromatography and the molecular structure can be fully characterized by ^{1}H NMR and mass spectra. Tian *et al.* prepared regioisomerically pure 1,6-dipyrrolidine PDI first and found that it presents significantly different properties from its 1,7 isomer.[33] Wasielewski compared the properties of 1,6- and 1,7-bis(*n*-octylamino)-substituted PDIs.[34] The electron paramagnanetic resonance (EPR) study together with the Density Functional Theory (DFT) calculation revealed that the substitution pattern strongly affects the electronic structure of the radical cations of these amine-substituted PDIs. Champness has successfully prepared 1,6- and 1,7-dimorpholino PDIs[35] and observed an unusual two-electron oxidation process for the 1,7-isomer.

Ever since the first time successful preparation of 1,7-dipyrrolidinyl or piperidinyl-substituted PDIs in 1999,[31] the significant differences on the absorption spectra between pyrrolidinyl- and piperidinyl-substituted PDIs were noticed but without further discussion. The large difference on the absorption spectra is interesting because of

* *Correspondence to: X. Li, Department of Chemistry, Shandong University, Jinan 250100, China.*
E-mail: xiyouli@sdu.edu.cn

a *J. Feng, D. Wang, H. Wang, D. Zhang, L. Zhang, X. Li*
Department of Chemistry, Shandong University, Jinan, China

b *J. Feng*
College of Shandong Policeman, Jinan, China

their very similar molecular structure. Further understanding on this difference might be helpful to reveal the origin of the effects of the bay substituents on the properties of PDI compounds. However, the detailed comparison between the properties of 1,7-dipyrrolidinyl- or piperidinyl-substituted PDIs has never been made. The present paper focuses on the difference of the structural and photophysical properties of the dipyrrolidinyl- or dipiperidinyl-substituted PDIs at 1,7 or 1,6 positions. For this purpose, four PDI compounds, namely, *N,N′* -dibutyl -1,7-dipyrrolidinyl-3,4:9,10-perylenetetra carboxylic diimide (**1**), *N,N′*-dibutyl-1,6-dipyrrolidinyl-3,4:9,10-perylene tetra carboxylic diimide (**2**), *N,N′*-dibutyl-1,7 -dipiperidinyl -3,4:9,10 -perylenetetra-carboxylic diimide (**3**), and *N,N′* -dibutyl -1,6-dipiperidinyl-3,4:9,10-perylene-tetra carboxylic diimide (**4**) were prepared (Scheme 1). The single crystals for 1,7-disubstituted compounds **1** and **3**, which are large enough for single crystal X-ray diffraction experiments, are obtained. The minor difference on the structure between pyrrolidine and piperidine leads to significant difference on the photophysical properties and bulky packing behavior between **1** and **3** as well as **2** and **4** as revealed in crystal structure and DFT calculation. We believe that the finding of this research will be helpful for the design of novel PDIs that maybe useful for molecular optoelectronic devices.

RESULTS AND DISCUSSION

Synthesis

The isomeric mixture *N,N′*-dibutyl-dibromo-3,4:9,10 -perylene -tetracarboxylic diimide was heated in pyrrolidine or piperidine to give the corresponding dipyrrolidinyl- or dipiperidinyl-substituted PDI isomeric mixture, respectively. The mixtures can be separated from each other by conventional column chromatography.[32,33] The structures of these compounds were fully characterized by different spectroscopic methods, including ^{1}H and ^{13}C NMR, MALDI-TOF mass spectrometry, and elemental analysis.

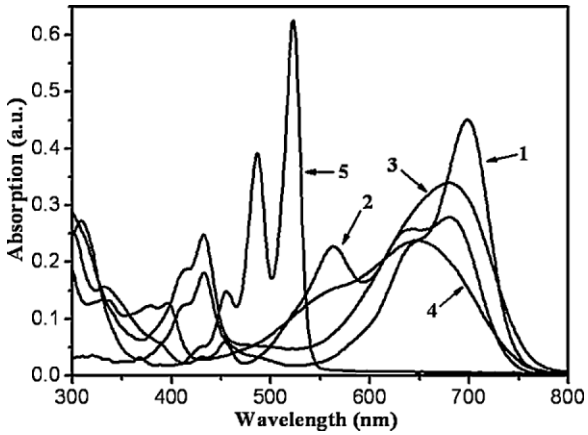

Figure 1. The absorption spectra of compounds **1**–**4** in CH_2Cl_2 compared with that of standard compound **5** in the same solvent (10^{-5}M)

UV–vis absorption

Figure 1 compares the electronic absorption spectra of compounds **1**–**4** with model compound *N,N′*-dibutyl-perylene -3,4:9,10-tetracarboxylic diimide (**5**) in dichloromethane. The measured spectral parameters are summarized in Table 1. All of these compounds show intense absorption in the UV–vis region. The maximum absorption band of compounds **1**, **2**, **3**, and **4** is red-shifted for about 175, 158, 157, 127 nm, respectively, relative to that of **5** because of the introduction of pyrrolidinyl or

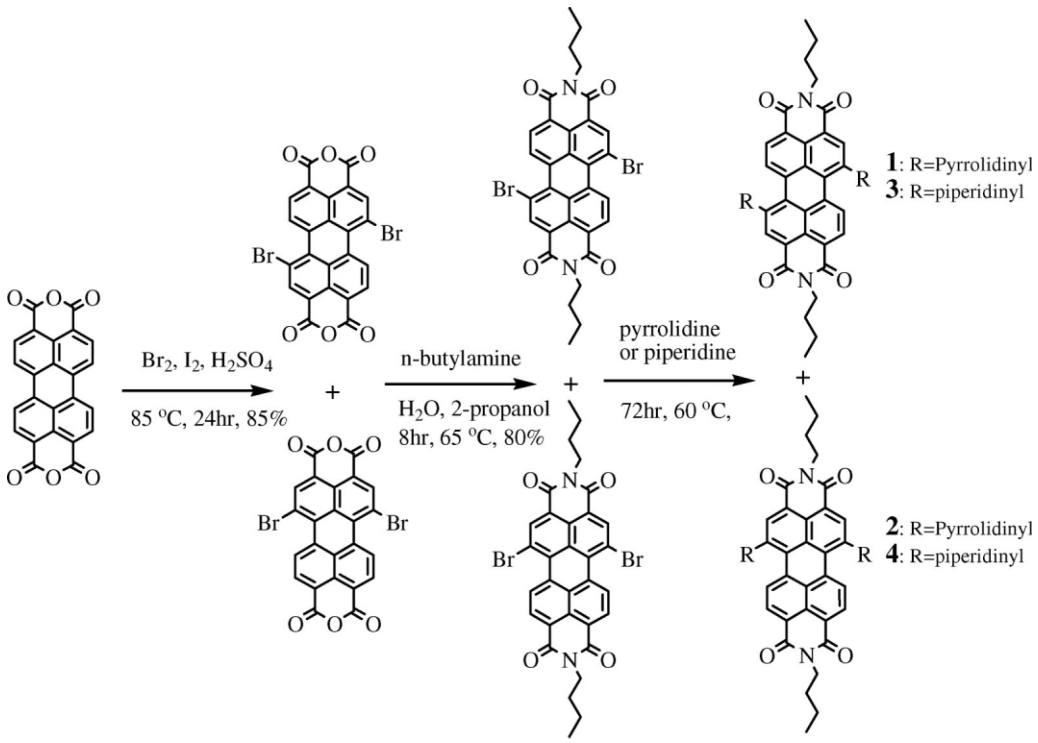

Scheme 1. Synthesis of compounds **1**–**4**

Table 1. The spectral parameters of compounds **1**–**4** and model compound **5**

Compounds		**1**	**2**	**3**	**4**	**5**
λ_{abs} (nm)		698	681	680	650	523
λ_{em} (nm)		739	735	757	761	532
$\Phi_{f\ (430)}$ (%)	Toluene	0.25	<0.01	0.015	<0.01	100
	THF	0.16	<0.01	0.016	<0.01	100
	CH_2Cl_2	0.79	0.05	0.08	<0.01	100
τ_f (ns)	Toluene	2.63	—	1.85	—	3.84
	THF	1.93	—	1.15	—	3.82
	CH_2Cl_2	1.98	—	1.23	—	3.82

piperidinyl group at the bay positions. It can be ascribed to the strong electron donating ability which promotes the conjugation of the entire molecule. Pyrrolidinyl or piperidinyl groups at the 1,6- and 1,7-positions of PDI show significantly different effect on the absorption spectra. The red-shift of the maximum absorption band of **1** is 17 nm larger than that of **2**, and similarly, the red-shift of **3** is 30 nm larger than that of **4**. In another word, the substitutents at 1,7 positions red-shifted the maximum absorption band more significantly than those at 1,6 positions. This might be attributed to the large degree distortion of the perylene core caused by the substituents at the 1,6-positions of PDI, which disturbs the conjugation system of PDI ring and thus brings small red-shift on the maximum absorption band.

Both pyrrolidine and piperidine are cyclic secondary amines, which have very similar structures. But pyrrolidinyl and piperidinyl group at the same position of PDI show evidently different effect on the absorption spectra as shown in Fig. 1 and Table 1. In compounds **1** and **3**, the pyrrolidinyl or piperidinyl groups are similarly connected at 1,7-positions of PDI ring, but the maximum absorption band of compound **1** is centered at about 698 nm, which red-shits for about 18 nm relative to that of compound **3**. Similarly, compound **2**, in which pyrrolidinyl groups are connected at 1,6 positions, presents a maximum absorption band at 681 nm, while compound **4** with piperidinyl groups substituted at the same positions show maximum absorption band at about 650 nm. The red-shift for the maximum absorption band of **2** is as large as 31 nm relative to that of **4**. These results indicate that pyrrolidinyl groups are more efficient on red-shift of the maximum absorption band than piperidinyl group. It is worth noting that cyclic primary amino groups substituted at 1,7 positions of PDI[34] can red-shift the maximum absorption band more efficiently than linear primary amino groups[36] attached at the same positions, suggesting that the steric hindrance might be an important source for this huge difference between the absorption spectra of pyrrolidinyl- and piperidinyl-substituted PDIs.

Fluorescence

The fluorescence spectra of these series compounds are recorded in dichloromethane with excitation at 430 nm. Fluorescence quantum yields (Φ_f) are calculated with model **5** as standard. The spectra and experimental results are summarized in Fig. 2 and Table 1. Similar to that observed for the absorption spectra, the maximum emission bands of compounds **1**–**4** red-shifted significantly relative to that of model **5**. This can be ascribed to the electron-donating properties of the pyrrolidine or piperidine units. The maximum emission bands of compounds **1**, **2**, **3**, and **4** are red-shifted for about 207, 203, 225, 229 nm, respectively, relative to that of **5**. Though the same substituents at the different positions of perylene bay region created significant different effect on the absorption spectra of the PDI isomers as mentioned above, but they did not show significant influence on their emission spectra. For example, the maximum emission wavelength of compound **1** with pyrrolidinyl groups at the 1,7-positions is only 4 nm longer than that of compound **2** with pyrrolidinyl group at the 1,6-positions. Similarly, difference of 4 nm between the maximum emission wavelength of compounds **3** and **4** was found, but with the 1,6-isomer **4** the longer wavelength emission was shown. Similar emission properties have also been found for a pair of linear amino groups substituted PDI isomers.[34]

Although the maximum absorption wavelengths of dipyrrolidinyl-substituted PDIs **1** and **2** are larger than that of dipiperidinyl-substituted PDIs **3** and **4**, but the maximum emission wavelengths of **1** and **2** are significantly shorter than that of **3** and **4**. This leads to large difference on their Stock's shifts between the dipyrrolidinyl- and dipiperidinyl-substituted PDIs. The Stock's shifts of dipyrrolidinyl-substituted PDIs are significantly smaller than that of dipiperidinyl-substituted PDIs. As the Stock's shift reflects directly the structure relaxing during the photo-excitation, larger Stock's shift corresponds to larger structure difference between the ground states and the excited states. Therefore, the smaller Stock's shift of **1** and **2** relative to those of **3** and **4** suggests that the structure relaxing during the

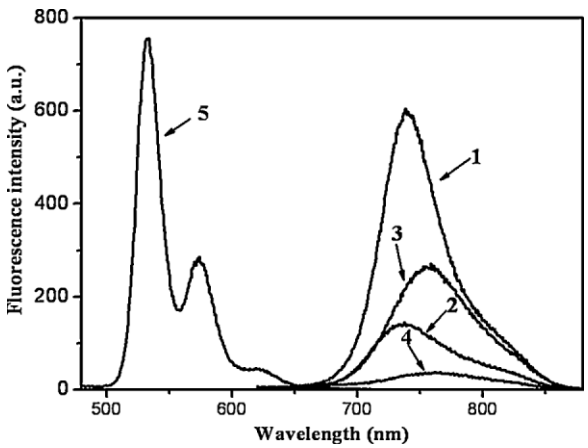

Figure 2. Fluorescence spectra of 1–4 compared with that of 5 in dichloromethane

photo-excitation of **1** and **2** are significantly smaller than those of **3** and **4**, which indicates that the molecular structure of **1** and **2** are more rigid than those of **3** and **4**.

The fluorescence quantum yields of compounds **1**, **2**, **3**, and **4** are distinctively smaller relative to that of standard compound **5** because of the introduction of pyrrolidine or piperidine. Due to the very strong electron-withdrawing nature of the PDI core, introducing electron-donating side groups onto the bay positions of the PDI core leads to charge transfer characteristic in the excited states of the PDI molecules, which in turn results in a significant decrease in the fluorescence quantum yield (Table 1). This corresponds well with the results found for other PDI compounds.[34,36] The fluorescence quantum yields of **1** and **3** are significantly larger than that of **2** and **4**. This might be attributed to the larger steric hindrance introduced by the side groups at 1,6 positions relative to that at 1,7 positions, which induce larger degree of distortion of the perylene core.[37] Compound **1** presents distinctively larger fluorescence quantum yields than compound **3**, which might be induced again by the more rigid molecular structure of compound **1** relative to **3** because of the different side groups as mentioned above. The rigid molecular structure could significantly reduce the proportion of nonradiative decay of the excited states through structure relaxing and, therefore, could increase the fluorescence quantum yields.

The fluorescence lifetimes of compounds **1** and **3** are shorter than that of standard compound **5** due to the electron transfer characteristic in the excited states. The measured fluorescence lifetimes are found to be sensitive to the solvent polarity. In polar solvents, the fluorescence lifetimes of **1** and **3** are reduced significantly probably because of the enhanced electron transfer characteristics of the excited states caused by the solvention. The fluorescence lifetimes of compounds **2** and **4** cannot be measured accurately because of the very weak emission intensity.

Electrochemical properties

The electrochemical behaviors of these compounds are investigated by cyclic voltammetry (CV) and differential pulse voltammetry (DPV). The half-wave redox potential values versus Saturated calomel electrode (SCE) of **1**–**4** together with that of model compound **5** are summarized in Table 2. Within the electrochemical window of CH_2Cl_2, these compounds undergo at least one reversible one-electron oxidation and reduction.

The introduction of pyrrolidinyl or piperidinyl groups at the positions of PDI bay region induces negative shift for first oxidation and reduction potentials of compounds **1**–**4**. This corresponds well to the electron-donating nature of pyrrolidinyl and piperidinyl groups. The negative shift of both first oxidation and reduction potentials of the compounds with pyrrolidinyl groups (**1** and **2**) are much more significant than that of the compounds with piperidinyl groups (**3** and **4**), which suggests again that the pyrrolidinyl groups interact with the perylene core more strongly than the piperidinyl groups connected at the same positions. The difference on the redox potentials between **1** and **3** as well as **2** and **4** revealed that the same group at different positions shows different effects on the redox potentials too. The side groups connected at 1,7 positions seem to be more efficient than the groups at 1,6 positions on negative shifting the oxidation or reduction potentials.

Table 2. Half-wave redox potentials[a] (mV vs. SCE) of **1**–**4** and **5** in CH_2Cl_2 containing 0.1 M TBAP

Compounds	Oxd_3	Oxd_2	Oxd_1	Red_1	Red_2	$\Delta E^\circ_{1/2}$[b]
1			0.75	−0.87	−1.00	1.62
2	1.65	1.21	0.85	−0.83	−0.97	1.68
3			0.86	−0.76	−0.96	1.62
4	1.91	1.43	0.97	−0.74	−0.95	1.71
5			1.63	−0.58	−0.82	2.21

[a] Values obtained by DPV in dry CH_2Cl_2 with 0.1 M TBAP as the supporting electrolyte and Fc/Fc^+ as internal standard.
[b] $E^\circ_{1/2} = Oxd_1 - Red_1$.

Crystal structure

For the purpose of deep understanding the relation between the molecular structure and the physical properties, the single crystals of compounds **1** and **3** suitable for X-ray diffraction analysis were grown by diffusion of methanol into a solution of **1** or **3** in CH_2Cl_2. Compound **1** belongs to C2c space group with calculated density $D_c = 1.208\ g/cm^3$ (Table S1, Supporting Information). The crystal structure of compound **1** is shown in Fig. 3A. The steric effect of two pyrrolidinyl substituents performs on the perylene core, leads to a twisting conformation for the two naphthalene subunits, and therefore, **1** gives a distorted molecular conformation. As a consequence, the characteristic torsion angles at the bay position of **1** are 20.18° (for C8-C9-C10-C11) and 20.05° (for C18-C19-C20-C1), which are in consistence with those observed for other substituted PDI derivatives.[35] The dihedral angle (α) of the two planes of the naphthalene subunit is 20.46° (Fig. 3B). The two pyrrolidinyl groups attached at the diagonal positions of the perylene core diminishes the symmetry to C_1 symmetry, leading to intrinsic chirality for the whole PDI molecule. The two enantiomers (Λ and Δ) with different chiral molecular conformation in mole ration 1:1 were observed in the crystal. The neighboring twisted molecules with the same chiral molecular conformation form a pseudo-dimer (Λ-Λ or Δ-Δ) in a clasp-like structure through intermolecular π–π interaction (Fig. 3B). It is worth noting that these two PDI molecules arranged is nonparallel with the dihedral angle (θ) of two planes through the axis atoms (N1-C21-C22-C23-C24-N2) of perylene cores amounting to 45.91° (Fig. 3C). This packing behavior is different from that previously reported for fluorinated PDIs[38] and can be assigned to the steric hindrance caused by the pyrrolidinyl groups. The cell unit of 1 contains eight PDI molecules (Fig. 3D). The adjacent pseudo-dimers are further linked by the intermolecular π–π interaction between the PDI core of the neighboring enantiotopic PDI molecules (Λ-Δ) separated in 3.39 Å, forming an infinite 1D chain-like supramolecular structure (-Λ-Λ-Δ-Δ-) (Fig. 3E).

The di-piperidinyl-substituted compound **3** crystallizes in triclinic system with $P-1$ space group. In comparison with the calculated density of **1**, the calculated density of **3** ($D_c = 1.192\ g/cm^3$) is slightly smaller, which may be ascribed to the looser packing mode than that of **1** as a result of the different side groups connected. As shown in Fig. 4A and B, there are two kinds of independent PDI molecules in the asymmetric unit due to the different bending direction of the piperidinyl groups. The characteristic torsion angles at the bay position of **3** are 20.06° (for C8-C9-C10-C11) and 17.38° (for C18-C19-C20-C1) in one PDI molecule and 18.09° (for C50-C51-C52-C53) and 18.22° (for

Journal of Physical Organic Chemistry

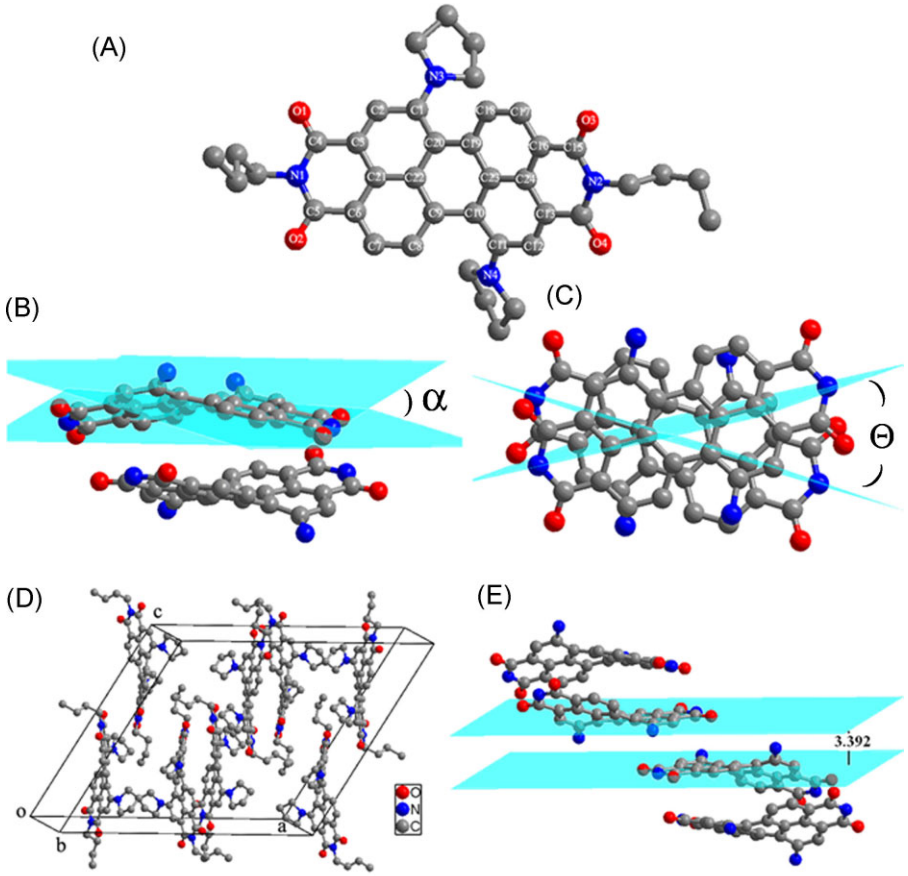

Figure 3. Single crystal structure of **1** with labels (A), pseudo-dimer (B and C), packing diagram (D), and side view on the stacks (E, only the perylene core is shown for clarity)

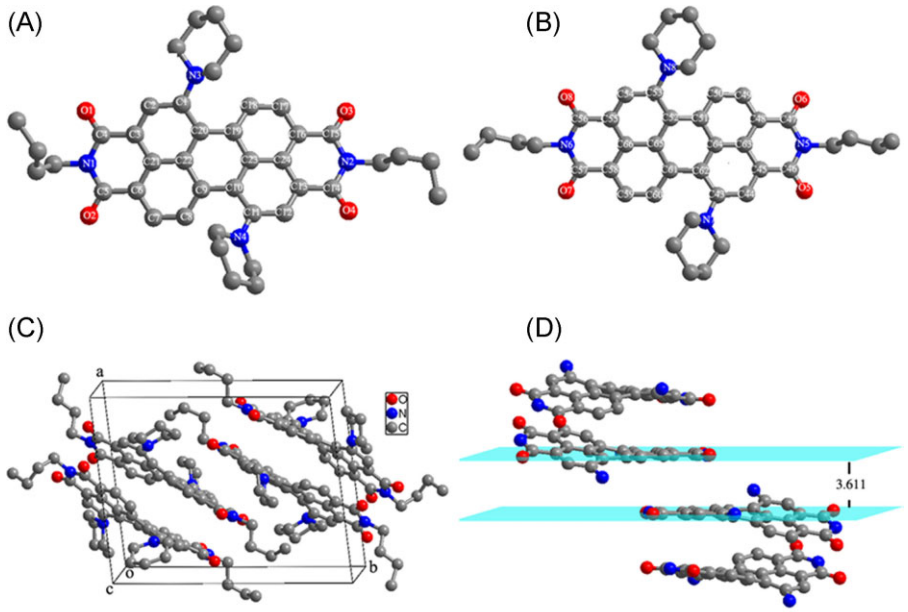

Figure 4. Single crystal structure of **3** with labels (A and B), packing diagram (C), and side view on the stacks (D, only the perylene part is shown for clarity)

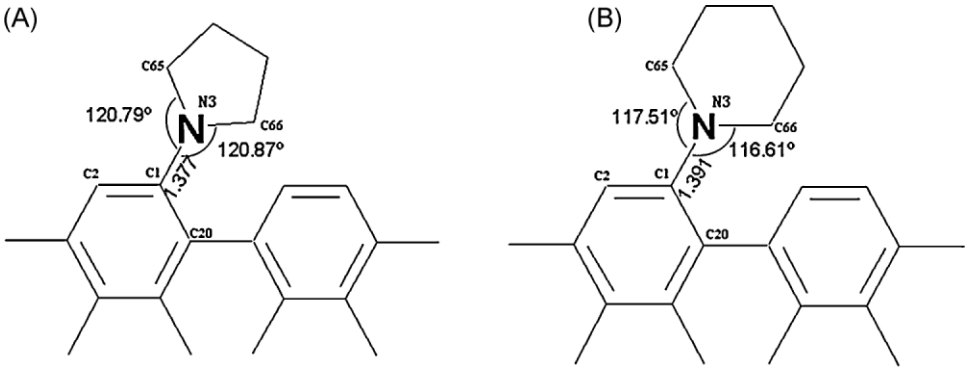

Figure 5. The bond length and bond angles around the nitrogen atom in compounds **1** (A) and **3** (B)

C60-C61-C62-C43) in the other one. The dihedral angle (α) of the two planes of the naphthalene subunits in **3** is 18.50° on average, which is slightly smaller than that observed for **1**, indicating that smaller steric hindrance from piperidinyl groups than that from pyrrolidinyl groups. Similar to compound **1**, intrinsic chirality for the whole PDI molecule is also found in **3**. The enantiomers Λ and Δ was observed in **3** in mole ratio 1:1. Despite the formed pseudo-dimers with $\theta = 32.22°$, the tetramer (Λ-Λ-Δ-Δ) bridged by the intermolecular π–π interaction between the neighboring PDI cores (Λ–Δ) separated in 3.61 Å are found in crystal of **3** instead of the 1D supramolecular chain of **1**, which may be assigned to the much bigger volume of piperidinyl groups than that of pyrrolidinyl groups.

As shown in Table S2 (Supporting Information), the bond length between C1 and N3 in compound **1** is 1.377 Å, which is distinctively smaller than that in compound **3** (1.391 Å). The measured bond angles of the bonds connected to the nitrogen atom of the pyrrolidinyl or piperidinyl groups in the crystal

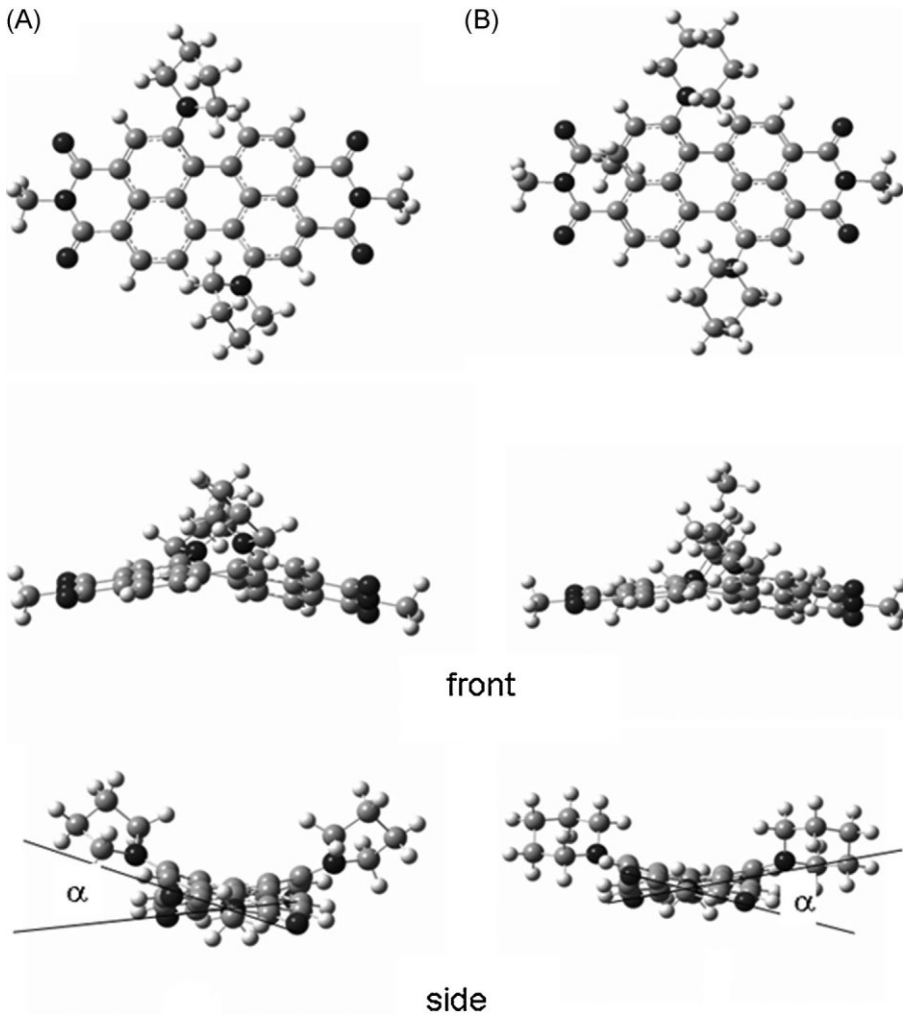

Figure 6. Minimized structures of compounds **1** (A) and **3** (B)

structures of **1** and **3** are shown in Fig. 5. In the five member ring of pyrrolidine in **1**, the bond angles between the bonds around the nitrogen atom are 120.87° and 120.79°, respectively. But in the six member ring of piperidine in compound **3**, the corresponding bond angles are 116.61° and 117.51°, which are smaller than those observed for compound **1**. So, nitrogen atoms of pyrrolidinyl groups of **1** have larger sp2 hybrid orbital characteristics, whereas nitrogen atoms of piperidinyl groups of **3** have more sp3 hybrid orbital characteristics, which suggests that there are double bond characteristics between C1 and N3 in compound **1** (Fig. 5A), otherwise, there are more single bond characteristics between C1 and N3 in compound **3** (Fig. 5B). Because the pyrrolidine group in compound **1** cannot rotate freely due to the double bond characteristic of C1—N3, it creates larger steric hindrance between the pyrrolidinyl group and the neighboring naphthalene ring of perylene core and, therefore, results in larger torsion angle between the two naphthalene subunits. All the structure characteristics as mentioned above indicate that the electron lone pair on the nitrogen atom in the pyrrolidinyl groups of **1** conjugated with the PDI core stronger than that in piperidinyl groups of **3**. This is in accordance with the conclusion deduced from the absorption and emission spectra as mentioned above.

DFT calculation

For the purpose of further understanding of the property–structure relation of PDI compounds, the molecular structures as well as the molecular orbital are calculated based on DFT method. The minimized molecular structures of compounds **1** and **3** are shown in Fig. 6. The minimized molecular structures correspond well to the crystal structure. For instance, the twist angle between the two naphthalene plans (α) in the calculated structure of **1** is 21.46°, which is similar to the measured result (20.46°). The calculated twist angle for **3** is 18.60°, which is also close to the measured twist angle (18.50°) in the crystal. The comparison results between the minimized structure and the crystal structure as mentioned above also suggest that the DFT calculation is reliable.

The frontier molecular orbital maps of compounds **1** and **3** are calculated at DFT/B3LYP/6–31g(d) level. Figure 7 shows the frontier orbital maps of **1** and **3** together with their energy levels as representative. The calculated energy gap between the HOMO and LUMO of **1** is 2.11 eV, which is slightly smaller than that of **3** (2.13 eV) as shown in Fig. 7. This is in accordance with the recorded red-shifted maximum absorption band of **1** relative to **3** in the absorption spectra. Both the HOMO and LUMO of **1** and **3** are extended successfully to the nitrogen atoms, indicating the contribution of the nitrogen atoms to the frontier molecular orbital and the interaction between the side groups and the PDI core. The contribution of nitrogen atom to the HOMO is obviously larger than that to the LUMO, which suggests that the nitrogen atom affected the HOMO more significantly than the LUMO; this has been proved by the fact that the introduction of side groups has induced more significant changes on the oxidation potentials than that on the reduction potentials, because the former is related closely with the HOMO while the later correlated with the LUMO closely.

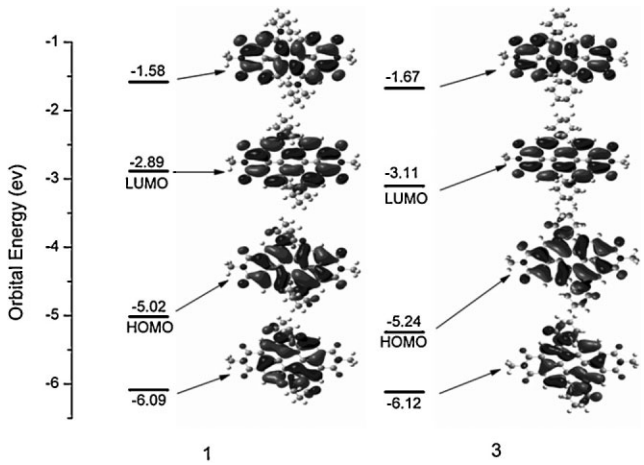

Figure 7. Frontier molecular orbital maps and energy levels of compounds **1** (left) and **3** (right)

CONCLUSION

Four PDI derivatives connected with cyclic amino groups at the bay positions were synthesized and the isomers with 1,7 and 1,6 substitution patterns were successfully separated by conventional column chromatography. Single crystals of the 1,7 disubstituted compounds (**1** and **3**) with proper size, which can be utilized in single crystal diffraction experiments, were obtained for the first time. The more double bond characteristics of C1—N3 in compound **1** relative to that in compound **3** caused stronger interactions between the pyrrolidinyl groups and the perylene core, which is the origin of the significantly different physical properties presented by compounds **1** and **3**. This information is meaningful not only for the design of novel PDI compounds, but also useful for the design of the new molecules with amino groups.

EXPERIMENTAL SECTION

^{1}H NMR spectra were recorded on a Bruker DPX 300 spectrometer (300 MHz) using $SiMe_4$ as reference. MALDI-TOF mass spectra were taken on a Bruker BIFLEX III mass spectrometer with α-cyano-4-hydroxycinnamic acid as the matrix. Electronic absorption spectra were recorded on a Hitachi U-4100 spectrophotometer, whereas the fluorescence spectra and fluorescence lifetime were recorded on ISIS K2 system. Elemental analyses were performed by the Institute of Chemistry, Chinese Academy of Sciences. Electrochemical measurements were carried out on a BAS CV-50W voltammetric analyzer with a glassy carbon disk working electrode (2.0 mm in diameter), a silver-wire counter electrode, and an Ag/Ag^+ reference electrode. The experiments were carried out under nitrogen at room temperature. Tetrabutylammonium perchlorate in freshly distilled CH_2Cl_2 (0.1 mol dm^{-3}) was used as the electrolyte solution. Ferrocene was employed as the reference redox system according to IUPAC's recommendation. Crystal data for these three complexes were collected on a Bruker SMART APEXII CCD diffractometer with graphite monochromatic Mo K_α radiation ($\lambda = 0.71073$ Å) using the SMART and SAINT programs at 298 K, and the structures were solved by the direct method (SHELXS-97) and refined by full-matrix least-squares (SHELXL-97) on F^2. Anisotropic thermal parameters were used for the nonhydrogen atoms and isotropic parameters for the hydrogen atoms. Hydrogen atoms were added geometrically and refined using

a riding model. Crystallographic data and other pertinent information for all the complexes are summarized in Table S1 (Supporting Information). Selected bond distances and their estimated standard deviations are listed in Table S2 (Supporting Information). CCDC 752512 and 752513 for **1** and **3**, respectively, contain the supplementary crystallographic data for this paper. These data can be obtained free of charge from the Cambridge Crystallographic Data Centre via www.ccdc.cam.ac.uk/data_request/cif.

N,*N*′-dibutyl-dibromo-3,4:9,10-perylene -tetracarboxylic diimide[39] and *N*,*N*′ -dibutyl-dibromo-3,4:9,10- perylene-tetracarboxylic diimide(**5**)[37] were prepared following the literature method and characterized by ^{1}H NMR, ^{13}C NMR, and MALDI-TOF mass spectra. Synthesis of compounds **1**–**4** is described in the following. All other chemicals are purchased from commercial source. Solvents were of analytical grade and were purified by the standard method before use.

***N*,*N*′-dibutyl-1,7-dipyrrolidinyl-3,4:9,10-perylenetetra-carboxylic diimide (1), and *N*,*N*′-dibutyl-1,6 -dipyrrolidinyl-3,4:9,10-perylenetetracarboxylic diimide (2)**: A mixture of *N*,*N*′-dibutyl-1,6-dibromo-3,4:9,10 -perylenetetracarboxylic diimide and *N*,*N*′ -dibutyl-1,7 -dibromo -3,4:9,10- perylenetetracarboxylic diimide (1 g, 1.51 mmol) was dissolved in 30 ml pyrrolidine. The solution was heated at 60° under dry nitrogen for 24 h with stirring. Excess pyrrolidine was removed on a rotary evaporator. The solid collected was purified by column chromatography on silica gel using $CHCl_3$ as eluent. **1**: green solid; 603 mg, yield 58%; mp. > 300 °C; ^{1}H NMR (300 MHz, $CDCl_3$) δ 8.37 (s, 2H), 8.31 (d, 2H), 7.53 (d, 2H), 4.24 (t, 4H), 3.68 (m, 4H), 2.76 (m, 4H), 1.99(m, 8H), 1.76(m, 4H), 1.48(m, 4H), 0.98 (t, 6H); ^{13}C NMR (100 Hz, $CDCl_3$) δ 164.0, 146.4, 134.1, 129.8, 126.6, 123.7, 122.1, 121.7, 120.7, 119.0, 118.0, 52.1, 40.3, 30.3, 25.8, 20.4, 13.9; MALDI-TOF MS(*m*/*z*) 640.8, Calcd for $C_{40}H_{40}N_4O_4$ (*m*/*z*) 640.8. Anal. Calcd. for $C_{40}H_{40}N_4O_4$: C, 74.98; H, 6.29; N, 8.74. Found: C, 74.95; H, 6.32; N, 8.71. **2**: blue solid; 156 mg, yield 15%; mp. > 300 °C; ^{1}H NMR (300 MHz, $CDCl_3$) δ 8.65 (d, 2H), 8.31 (s, 2H), 7.85 (d, 2H), 4.23 (m, 4H), 3.68 (m, 4H), 2.77 (m, 4H), 2.00(m, 8H), 1.76(m, 4H), 1.49(m, 4H), 0.98 (t, 6H); ^{13}C NMR (100 Hz, $CDCl_3$) δ 164.3, 164.1, 149.9, 135.7, 131.1, 130.2, 128.5, 128.3, 123.3, 122.9, 117.8, 117.6, 117.0, 116.9, 52.1, 40.3, 40.2, 30.4, 30.3, 25.6, 20.5, 20.4, 13.9, 13.8; MALDI-TOF MS(*m*/*z*) 640.8, Calcd for $C_{40}H_{40}N_4O_4$ (*m*/*z*) 640.8. Anal. Calcd. for $C_{40}H_{40}N_4O_4$: C, 74.98; H, 6.29; N, 8.74. Found: C, 74.93; H, 6.35; N, 8.72.

***N*,*N*′-dibutyl-1,7-dipiperidinyl-3,4:9,10-perylenetetra-carboxylic diimide (3), and *N*,*N*′-dibutyl-1,6-dipiperidinyl-3,4:9,10 -perylenetetracarboxylic diimide (4)**: A mixture of *N*,*N*′-dibutyl-1,6-dibromo-3,4:9,10- perylenetetracarboxylic diimide and *N*,*N*′-dibutyl-1,7-dibromo -3,4:9,10 -perylenete tracarboxylic diimide (1 g, 1.51 mmol) was dissolved in 30 ml piperidine. The solution was heated at 60° under dry nitrogen for 48 h with stirring. Excess piperidine was removed on a rotary evaporator. The solid collected was purified by column chromatography on silica gel using 1:2 CH_2Cl_2/CCl_4 as eluent. **3**: green solid; 619 mg, yield 61%; mp. > 300 °C; ^{1}H NMR (300 MHz, $CDCl_3$) δ 9.29 (d, 2H), 8.24 (d, 2H), 8.17 (s, 2H), 4.24 (t, 4H), 3.34 (d, 4H), 2.76 (m, 4H), 1.36–1.88(m, 20H), 0.99 (t, 6H); ^{13}C NMR (100 Hz, $CDCl_3$) δ 163.4, 163.3, 150.5, 134.9 129.4, 127.6, 123.7, 123.3, 122.9, 122.3, 122.2, 120.6, 52.6, 40.4, 32.4, 30.3, 25.7, 23.8, 20.5, 13.9; MALDI-TOF MS(*m*/*z*) 668.8, Calcd for $C_{42}H_{44}N_4O_4$ (*m*/*z*) 668.8. Anal. Calcd. for $C_{42}H_{44}N_4O_4$: C, 75.42; H, 6.63; N, 8.38. Found: C, 75.39; H, 6.62; N, 8.41. **4**: blue solid; 142 mg, yield 14%; mp. > 300 °C; ^{1}H NMR (300 MHz, $CDCl_3$) δ 9.71 (d, 2H), 8.58 (d, 2H), 8.36 (s, 2H), 4.20 (m, 4H), 3.35 (d, 4H), 2.85 (m, 4H), 1.40–1.91(m, 20H), 0.98 (m, 6H); ^{13}C NMR (100 Hz, $CDCl_3$) δ 163.8, 163.7, 153.2, 136.0, 131.7, 130.7, 128.8, 128.0, 123.8, 123.2, 123.1, 122.3, 120.7, 120.2, 53.1, 40.3, 40.2, 30.3, 30.2, 25.8, 23.8, 20.5, 20.4, 13.9, 13.8; MALDI-TOF MS(*m*/*z*) 668.8, Calcd for $C_{42}H_{44}N_4O_4$ (*m*/*z*) 668.8. Anal. Calcd. for $C_{42}H_{44}N_4O_4$: C, 75.42; H, 6.63; N, 8.38. Found: C, 75.38; H, 6.61; N, 8.43.

Acknowledgements

The authors acknowledge the financial support from the natural science foundation of China (grant no. 20771066 and 20640420467), Ministry of education.

REFERENCES

[1] M. R. Wasielewski, *J. Org. Chem.* **2006**, *71*, 5051–5066.
[2] J. A. A. W. Elemans, R. Van Hameren, R. J. M. Nolte, A. E. Rowan, *Adv. Mater.* **2006**, *18*, 1251–1266.
[3] H. Langhal, *Helv. Chim. Acta.* **2005**, *88*, 1309–1343.
[4] F. Würthner, *Chem. Commun.* **2004**, 1564–1579.
[5] E. Yukruk, A. L. Dogan, H. Canpinar, D. Guc, E. U. Akkaya, *Org. Lett.* **2005**, *7*, 2885–2887.
[6] M. Berberich, A.-M. Krause, M. Orlandi, F. Scandola, F. Würthner, *Angew. Chem. Int. Ed. Engl.* **2008**, *47*, 6616–6619.
[7] K. Sugiyasu, N. Fujita, S. Shinkai, *Angew. Chem. Int. Ed. Engl.* **2004**, *43*, 1229–1233.
[8] B. Rybtchinski, L. E. Sinks, M. R. Wasielewski, *J. Am. Chem. Soc.* **2004**, *126*, 12268–12269.
[9] Y. Shibano, T. Umeyama, Y. Matano, H. Imahori, *Org. Lett.* **2007**, *9*, 1971–1974.
[10] Y. Shibano, H. Imahori, C. Adachi, *J. Phys. Chem. C* **2009**, *113*, 15454–15466.
[11] T. Edvinsson, C. Li, N. Pschirer, J. Schöneboom, F. Eickemeyer, R. Sens, G. Boschloo, A. Herrmann, K. Müllen, A. Hagfeldt, *J. Phys. Chem. C* **2007**, *111*, 15137–15140.
[12] Y. Jin, J. Hua, W. Wu, X. Ma, F. Meng, *Synth. Met.* **2008**, *158*, 64–67.
[13] C. Hippius, F. Schlosser, M. O. Vysotsky, V. Böhmer, F. Würthner, *J. Am. Chem. Soc.* **2006**, *128*, 3870–3871.
[14] W. S. Shin, H.-H. Jeong, M.-K. Kim, S.-H. Jin, M.-R. Kim, J.-K. Lee, J. W. Lee, Y.-S. Gal, *J. Mater. Chem.* **2006**, *16*, 384–390.
[15] Y. Shibano, T. Umeyama, Y. Matano, N. V. Tkachenko, H. Lemmetyinen, Y. Araki, O. Ito, H. Imahori, *J. Phys. Chem. C* **2007**, *111*, 6133–6142.
[16] L. Chen, J. H. Yum, S.-J. Moon, A. Herrmann, F. Eickemeyer, N. G. Pschirer, P. Erk, J. Schöneboom, K. Müllen, M. Grätzel, M. K. Nazeeruddin, *ChemSusChem.* **2008**, *1*, 615–618.
[17] Y. Shibano, T. Umeyama, Y. Matano, N. V. Tkachenko, H. Lemmetyinen, H. Imahori, *Org. Lett.* **2006**, *8*, 4425–4428.
[18] H. Langhals, S. Kirner, *Eur. J. Org. Chem.* **2000**, 365–380.
[19] A. S. Lukas, Y. Zhao, S. E. Miller, M. R. Wasielewski, *J. Phys. Chem. B* **2002**, *106*, 1299–1306.
[20] J. M. Giaimo, A. V. Gusev, M. R. Wasielewski, *J. Am. Chem. Soc.* **2002**, *124*, 8530–8531.
[21] M. J. Fuller, L. E. Sinks, B. Rybtchinski, J. M. Giaimo, X. Y. Li, M. R. Wasielewski, *J. Phys. Chem. A* **2005**, *109*, 970–975.
[22] T. M. Wilson, M. J. Tauber, M. R. Wasielewski, *J. Am. Chem. Soc.* **2009**, *131*, 8952–8957.
[23] J. Mareda, S. Matile, *Chem. Eur. J.* **2009**, *15*, 28–37.
[24] A. Perez-Velasco, V. Gorteau, S. Matile, *Angew. Chem. Int. Ed. Engl.* **2008**, *47*, 921–923.
[25] W. S. Shin, H.-H. Jeong, M.-K. Kim, M.-R. Kim, M.-K. Kim, B. V. K. Naidu, S.-H. Jin, J.-K. Lee, J. W. Lee, Y.-S. Gal, *Mol. Cryst. Liq. Cryst.* **2007**, *462*, 59–66.
[26] J. Fuller, M. C. J. Walsh, Y. Zhao, M. R. Wasielewski, *Chem. Mater.* **2002**, *14*, 952–953.
[27] J. Feng, Y. Zhang, C. Zhao, R. Li, W. Xu, X. Li, J. Jiang, *Chem. Eur. J.* **2008**, *14*, 7000–7010.
[28] J. Feng, B. Liang, D. Wang, H. Wu, L. Xue, X. Li, *Langmuir* **2008**, *24*, 11209–11215.

[29] M. Franceschin, A. Alvino, G. Ortaggi, A. Bianco, *Tetrahedron Lett.* **2004**, *45*, 9015–9020.
[30] J. Fortage, M. Séverac, C. Houarner-Rassin, Y. Pellegrin, E. Blart, F. Odobel, *J. Photochem. Photobiol. A: Chem.* **2008**, *197*, 156–169.
[31] Y. Zhao, M. R. Wasielewski, *Tetrahedron Lett.* **1999**, *40*, 7047–7050.
[32] F. Würthner, V. Stepanenko, Z. J. Chen, C. R. Saha-Möller, N. Kocher, D. Stalke, *J. Org. Chem.* **2004**, *69*, 7933–7939.
[33] L. Fan, Y. Xu, H. Tian, *Tetrahedron Lett.* **2005**, *46*, 4443–4447.
[34] M. J. Ahrens, M. J. Tauber, M. R. Wasielewski, *J. Org. Chem.* **2006**, *71*, 2107–2114.
[35] G. Goretzki, E. S. Davies, S. P. Argent, W. Z. Alsindi, A. J. Blake, J. E. Warren, J. McMaster, N. R. Champness, *J. Org. Chem.* **2008**, *73*, 8808–8814.
[36] C. Zhao, Y. Zhang, R. Li, X. Li, J. Jiang, *J. Org. Chem.* **2007**, *72*, 2402–2410.
[37] Y. O. Su, K.-Y. Chiu, T.-H. Lin, *J. Org. Chem.* **2005**, *70*, 4323–4331.
[38] R. Schmidt, J. H. Oh, Y.-S. Sun, M. Deppisch, A. M. Krause, K. Radacki, H. Braunschweig, M. Könemann, P. Erk, Z. Bao, F. Würthner, *J. Am. Chem. Soc.* **2009**, *131*, 6215–6228.
[39] H. Langhals, W. Jona, *Eur. J. Org. Chem.* **1998**, 847–851.